ELSEVIER

Journal of Chromatography A, 836 (1999) 129–136

JOURNAL OF CHROMATOGRAPHY A

Dynamic computer simulations of the influence of injection conditions on capillary zone electrophoretic stacking of preparative free-flow zone electrophoresis fractions of peptides

Jetse C. Reijenga[a,*], Václav Kašicka[b]

[a]*Laboratory of Instrumental Analysis, University of Technology, P.O. Box 513, 5600 MB Eindhoven, The Netherlands*
[b]*Institute of Organic Chemistry and Biochemistry, Academy of Sciences of the Czech Republic, Flemingovo 2, 166 10 Prague 6, Czech Republic*

Abstract

Dynamic computer simulations were carried out to investigate the effect of residual acetic acid content on the initial stacking conditions of oligoglycine samples during the analytical CE run. These simulations were carried out with both individual peptides and with their equimolar mixtures. Results indicate that optimum acetic acid conditions were in the range of equimolar values.

Keywords: Computer simulation; Injection methods; Stacking; Peptides

1. Introduction

Mixtures of synthetic oligopeptides, e.g. oligoglycines, were separated by preparative free-flow zone electrophoresis (FFZE) using 0.5 mol/l acetic acid as the background electrolyte (BGE). Collected fractions of separated peptides were lyophilized and their purity was tested by capillary zone electrophoresis (CZE) in the same BGE as in FFZE. During the lyophilization most of acetic acid is removed but depending on the basicity of separated peptides and lyophilization procedure different amounts of residual acetic acid remain bound to peptides as counterion. The content of the acetic acid in the peptide sample influences the initial stacking conditions of CZE analysis of FFZE peptide fractions.

1.1. Stacking phenomena

The process of stacking in capillary electrophoresis comprises one of the major advantages of the separation technique with respect to chromatographic separation methods [1–6]. Some rules-of-thumb for stacking will make this clear. Essential is the phenomenon described by Kohlrausch's regulating function [7]. If the sample is dissolved in the background electrolyte, there is no stacking or concentration adjustment on the border between sample and the separation compartment after switching on the voltage. The initial concentration equals the original sample concentration. If the ionic strength (or conductivity) of the injected solution is larger than that of the BGE, concentration adjustment will lead to a lower concentration, i.e. a dilution, de-stacking. If on the other hand, the sample solution introduced has a low concentration (ionic strength, conductivity), and consequently higher field strength, stacking will locally increase the concentration of the sample

*Corresponding author. Tel.: +040-247-30-96; fax: +040-245-37-62; e-mail: j.c.reijenga@tue.nl

0021-9673/99/$ – see front matter
PII: S0021-9673(98)00982-0

components. The maximum concentration finally obtained (in general within a fraction of a second), governed by the Kohlrausch function, will have a value generally approaching the co-ion concentration in the BGE.

1.2. Definition of a stacking factor

Estimates of stacking factors can be made by looking at the properties of the sample, as present in the sample compartment. For a quantitative assessment of the phenomenon, a stacking factor can be defined in different ways:

1. the ratio of the initial linear velocity in the sample compartment and that in the BGE
2. the ratio of the maximum concentration (any time, anywhere) and the initial concentration in the sample.

It is obvious that the first, velocity based definition requires only information about the initial conditions in the sample, plus the detection signal. If we assume the effective mobilities in the sample compartment to be equal to those in the BGE (a realistic approximation only for strong ions), the above mentioned velocity ratio equals the ionic strength ratio or more precisely the field strength ratio between sample solution and BGE. Diluting the sample and injecting a correspondingly larger volume will sometimes be advantageous for this reason, with limitations.

The second, concentration based definition, in addition requires dynamic simulation. The reason for this is that mutual interaction of all components in the sample solution takes place. The local field strength in the sample compartment changes during the stacking process, and local pH changes can lead to locally different effective mobilities.

2. Materials and methods

2.1. Experimental conditions

The FFZE experiments [8] were performed in a chamber of two parallel glass plates of 500×500 mm, with a 0.5 mm gap in between, a sample flow rate of 1.5 ml/h. Both sides were air-cooled at −1°C. The separation voltage was 3000 V, resulting in a current of 125 mA using 0.5 *M* acetic acid (pH 2.5) as a BGE. From the outlet of the separation chamber, 48 fractions were collected and off-line measured at 225 nm.

Analyses were performed in home-made CZE equipment [9] with a fused silica capillary of 300 mm (length to the detector 200 mm)×56 μm I.D.× 200 μm O.D., 8 kV positive polarity, operating temperature 23.5°C. Passive air-cooling was used. Hydrostatic injection was applied for 12 s, height difference 50 mm (injection length ca. 1 mm). Detection wavelength was 206 nm. Background electrolyte was 0.5 *M* acetic acid (pH 2.5).

2.2. Simulation conditions

The dynamic simulation model was a one-dimensional migration–diffusion model, without temperature and ionic strength correction. Several authors have, in recent years, published on numerical simulation in CE and ITP [5,10–18].

Our previously published simulation program [18] solves the one dimensional migration diffusion differential equation using a number of different numerical approaches. It appeared that depending on the situation, each time a compromise needs to be found between numerical diffusion (unrealistically fast levelling-out of concentration gradients due to the numerical algorithm) and numerical oscillations (leading to artifacts such as negative concentrations, mass balance violations and general run-away of the calculations). The numerical algorithm was DIME [18], where diffusion is taken implicitly in a second-order central difference scheme and migration explicitly with a first order upwind scheme. This algorithm combines a high calculation speed and reasonable numerical stability with a usually acceptable degree of numerical diffusion [18].

Simulated conditions were the same as experimental conditions with the exception of constant driving current, instead of constant voltage. Injection length was variable and electroosmotic flow (EOF) was suppressed.

Steady-state simulations [19,20] were carried out using the literature data of p*K* values [21] and mobilities [22,23] for sample and buffer components. In contrast with the dynamic simulation, mutual interaction of components and diffusion were not taken into account. Corrections for ionic strength and

Table 1
Mobility and pK data of oligoglycines and acetic acid, at $c=0$ and $T=25$°C

Component	μ_0	pK_1	μ_1	pK_2	μ_2
Acetic acid	0	4.76	−42.4	–	–
Diglycine	31.5	3.12	0	8.17	−31.5
Triglycine	26.1	3.26	0	7.91	−26.1
Tetraglycine	23.3	3.05	0	7.75	−23.3
Pentaglycine	21.2	3.05	0	7.70	−21.2
Hexaglycine	19.3	3.05	0	7.60	−19.3

temperature were made however. The pK and mobility values used in the simulations are given in Table 1.

3. Results and discussion

3.1. Steady-state simulations

Simulation of a mixture of 10^{-4} M each of di-, tri-, tetra-, penta- and hexaglycine dissolved in BGE. The simulation conditions were equal to the experimental conditions. Experimental electropherograms were obtained from a mixture of 10^{-4} M each of diglycine and triglycine, dissolved in BGE. Phenol was used as an EOF marker. Using the external radial electric field at different values, different zeta potentials and consequently different EOF values were obtained, see Table 2. An example of an experimental and a simulated electropherogram is given in Fig. 1a and 1b, respectively. There is a slight difference in migration time, where we have to consider that the experimental temperature was not so well defined because of the air-cooling. Calculations have revealed that the temperature-rise inside the capillary (due to Joule heating) can be several degrees, depending on the effectiveness of the air-cooling.

Table 2
Effect of external field on EOF

V_{rad} (V)	t_{EOF} (min)	ζ (mV)
Off	6.5	−24
−6000	5.3	−30
−8000	4.8	−33

3.2. Initial conditions

In the first example, suppose we take a 10^{-4} M solution of tetraglycine with different acetic acid concentrations. In addition, we take a mixture of five oligoglycines. In both cases the initial field strength, and effective mobility and linear velocity of tetraglycine, just prior to switching on the power, were calculated.

In both cases there are counteracting effects, illustrated by Fig. 2. A low acetic acid concentration will decrease the conductivity in the sample compartment and thus increase the field strength. On the other hand, a low acetic acid concentration will increase the pH in the sample compartment and thus decrease the charge and consequently the effective mobilities. As a result of these effects, the initial linear velocity, being the product of the field strength and the effective mobility, will show an optimum value. This is the case both for the single peptide and for tetraglycine in a five component mixture. Consider that the linear velocity of tetraglycine in the BGE is 0.607 mm/s (at ''zero'' sample concentration), the ratio of the initial and ultimate velocity is thus ca. 4.

3.3. Dynamic simulation of tetraglycine

Without simulation, the first, velocity-based definition of the stacking factor yielded a value of ca. 4. It remains to be seen if the stacking factor using the second definition yields the same result. This is because with the second definition we take into account the accumulative behaviour of the sample component during the stacking period, until approximately the time when most of the sample will have left the injection compartment.

A solution of 10^{-4} M tetraglycine with acetic acid in the range 250 μM and 500 mM was simulated with an injection length of 1000 μm. Maximum tetraglycine concentration in time was reached at low acetic acid concentration around 500 ms, somewhat later at higher acetate concentrations. All cases were

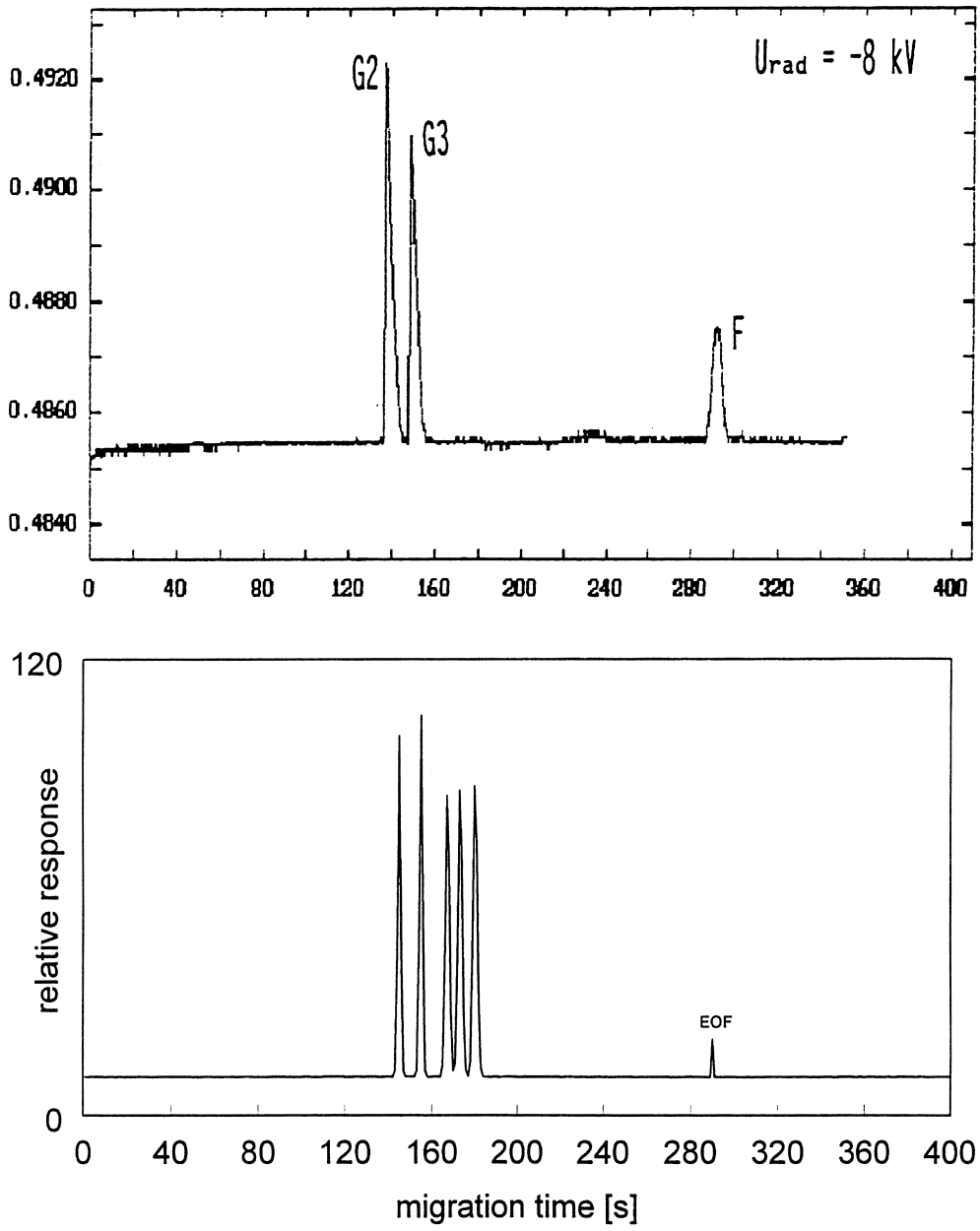

Fig. 1. Experimental and simulated electropherogram of a mixture of 2 and 5 oligoglycines respectively. See text for further details

simulated for 500 ms for this reason. Results are shown in Fig. 3. Differences in extent to which the sample component has left the sample compartment are due to sample matrix dependence of tetraglycine transport number, this number obviously decreasing at higher acetate concentrations. This illustrates one of the possible explanations why the migration time may sometimes depend on the sample composition.

The sample pH and the stacked, adjusted maximum (plateau) concentration were plotted vs. the

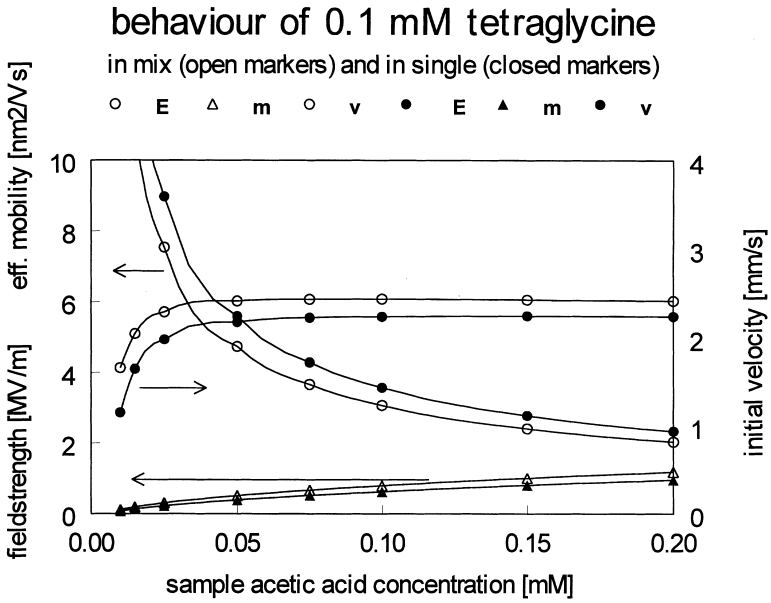

Fig. 2. Initial values for the local field strength *E*, effective mobility *m* and linear velocity *v* of tetraglycine in a mixture and in a single solution of 0.1 m*M* concentration as a function of the acetic acid concentration in the sample.

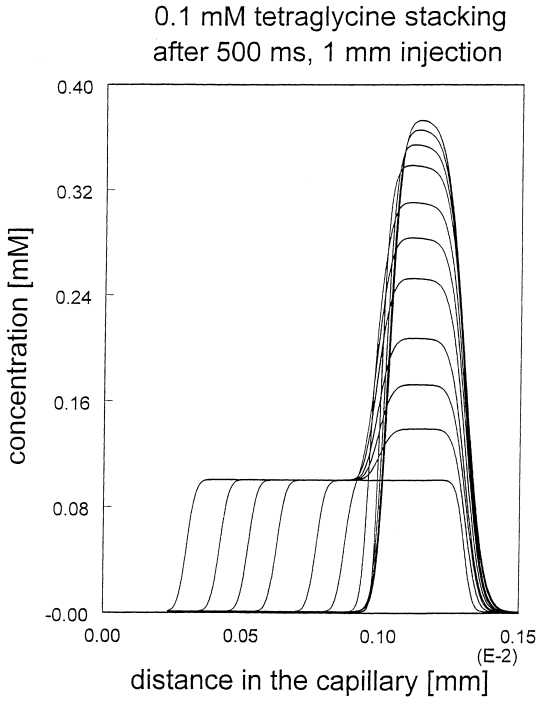

Fig. 3. Concentration profile of 0.1 m*M* tetraglycine after 500 ms of simulation as a function of the acetic acid concentration in the sample, ranging from 250 μ*M* to 500 m*M*. See text for further explanation.

acetic acid concentration in Fig. 4. Maximum stacking factor approaching four, but ultimately limited by higher sample pH, as outlined in a previous section. At acetate concentrations >1 m*M*, a plateau value of the tetraglycine concentration was initially obtained outside the sample compartment, suggesting Kohlrausch-law adjustment. Although the Kohlrausch regulating function (KRF) in the background electrolyte did not deviate from the value of $11.80 \cdot 10^{+9}$ kmol V s/m^5, the adjusted tetraglycine concentration just outside the injection compartment depended on the acetic acid concentration inside the injection compartment, in itself an unusual phenomenon. We have to consider that under these conditions, equal values for KRF functions can likely be achieved with different tetraglycine concentration–pH combinations. These pH changes were found to be very small, in the third decimal. But as the transport number of the hydrogen ions is expected to be high, this can nevertheless account for the effect that the specific conductivity of the BGE, due to the stacking of the sample, decreases from 111.3 mS/m to 107.7 mS/m at the highest stacking factor (at the lowest acetic acid concentration of 0.25 m*M*). The specific conductivity after stacking, just like the tetraglycine

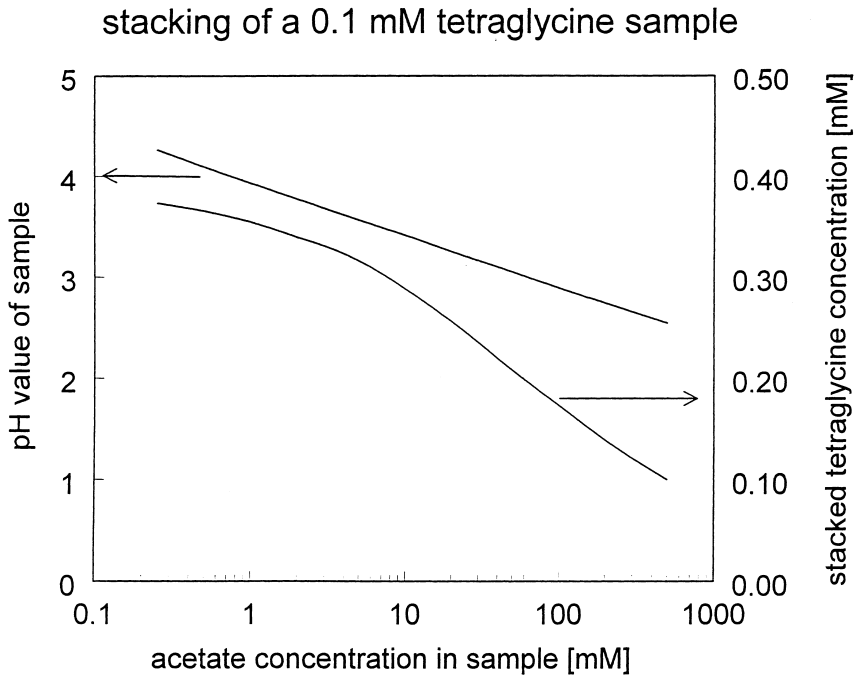

Fig. 4. Sample pH and stacked tetraglycine concentration as a function of the acetic acid concentration in the sample. The tetraglycine concentration in the sample was 0.1 m*M*. Note the logarithmic scale of the *x*-axis.

concentration, thus depends on the acetic acid concentration in the sample (injection compartment).

3.4. Time-development of the tetraglycine concentration

A 10^{-4} *M* tetraglycine solution was analyzed with 0.250 m*M* acetic acid, in a 1000 μm injection plug, after a simulation time of respectively 100, 200, 300, 400, 500, 500, 600, 800 and 1000 ms. As soon as the sample component is outside the sample compartment, the process of diffusion sets in, resulting in a decrease of the peak maximum concentration. See Fig. 5 for the concentration profiles.

3.5. Numerical diffusion

Numerical diffusion was mentioned as an uncertainty factor in numerical simulation of CZE in only some of the references cited on the subject. The degree of numerical diffusion, as a relative contribution, was estimated by simulating an example with different Peclet (Pe) numbers, defined as $Pe = v.dz/D$, in which v is the linear velocity, dz the grid size and D the diffusion coefficient. The Pe number for each component in the system can have different values at any time and at any location in the capillary. Previous work [18] revealed that numerical diffusion increases with increasing maximum Peclet number. The problem arises that in order to lower the Peclet number for a given set of experimental conditions (v/D), the grid size dz has to be refined (decreased), thus increasing the calculation time proportionally. The example to illustrate this is the stacking of 10^{-4} *M* tetraglycine with 0.25 m*M* acetic acid, a 1000 μm length injection plug during 500 ms. Initial grid size dz was 1 μm and 8 μm, resulting in maximum Pe numbers of 17 and 136, respectively. As depicted in Fig. 6, the resulting difference is significant but has no effect on the concentration plateau values calculated.

3.6. Dynamic simulation of a mixture

A mixture of 10^{-4} *M* each of diglycine up to hexaglycine was now simulated with different acetic

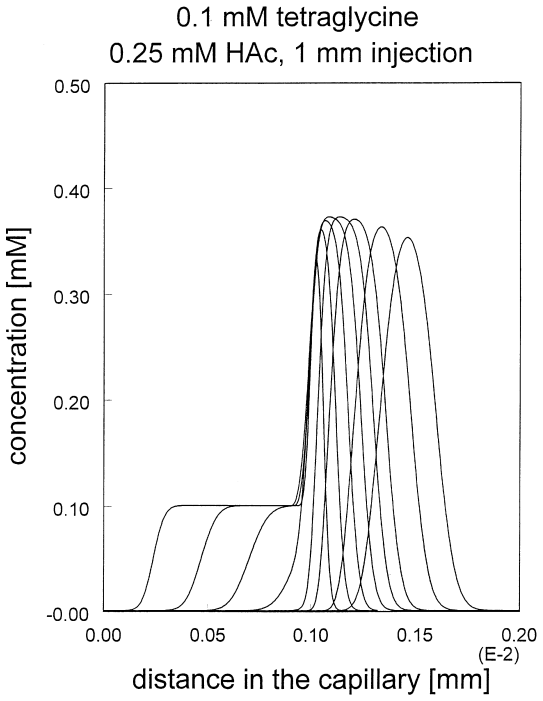

Fig. 5. Concentration profile of a 0.1 m*M* tetraglycine sample (injection length 1 mm) containing 250 μ*M* acetic acid, after 100, 200, 300, 400, 500, 600, 800 and 1000 ms respectively.

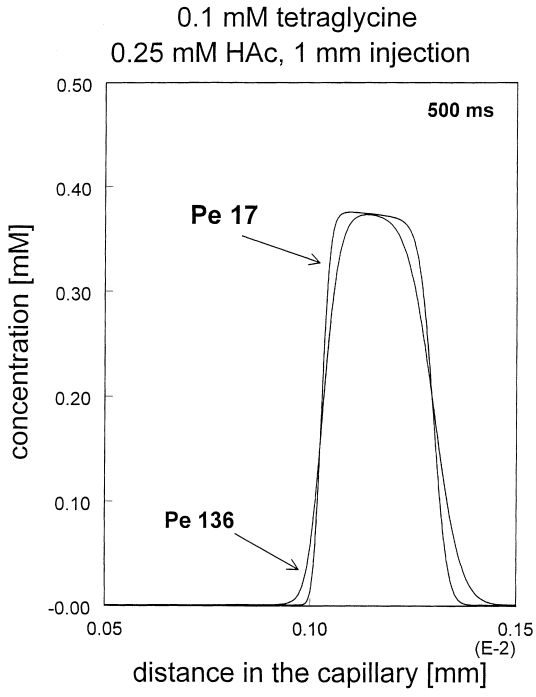

Fig. 6. Simulated concentration profiles after 500 ms of a 1000 μm injection plug of 0.1 m*M* tetraglycine with 0.25 m*M* acetic acid, using grid size 1 μm (Pe 17) and 8 μm (Pe 136) respectively.

acid concentrations, 100 μm plug length, 30 ms simulation time. The results with 100, 250, 500 and 1000 μ*M* acetic acid do not show much difference. See Fig. 7 for the 250 μ*M* results.

Less (physical and numerical) diffusion takes place on a scale of 1000 μm injection plug, after 500 ms, with acetic acid concentrations between 0.5 m*M* and 10 m*M*. The value of 0.5 m*M* acetic acid gives the best stacking performance, a factor approaching the value of 4.

Although the concentration of the background electrolyte is rather high, the ionic strength is relatively low and determined by the proton concentration: 0.0316 mol/l. If the buffer cation is anything but the proton, one would expect the stacking factor, according to the second definition, to be as large as several hundred, according to Kohlrausch-law adjustment in isotachophoresis. But with the proton as a (leading) co-ion, things are not that predictable. Experimental verification using ITP with 500 m*M* acetic acid as a leading electrolyte is impossible [2–4]. Then, we have to keep in mind that the Kohlrausch regulating function for weak ions is less straightforward than for strong ions.

4. Conclusions

Best stacking conditions for 10^{-4} *M* oliglycines are obtained with around equimolar acetic acid concentrations. The pH and field strength in the sample compartment play an important role. A low acetate concentration increases the pH, thus decreasing the effective mobilities. A high acetate concentration will decrease the field strength in the sample compartment. A stacking factor of approximately four is found under optimized conditions. Conveniently enough, in this case, two different definitions of the stacking factor yield approximately the same results. It was shown that for weak ions, sample pH could be a constraint on the stacking factor in dilute solutions.

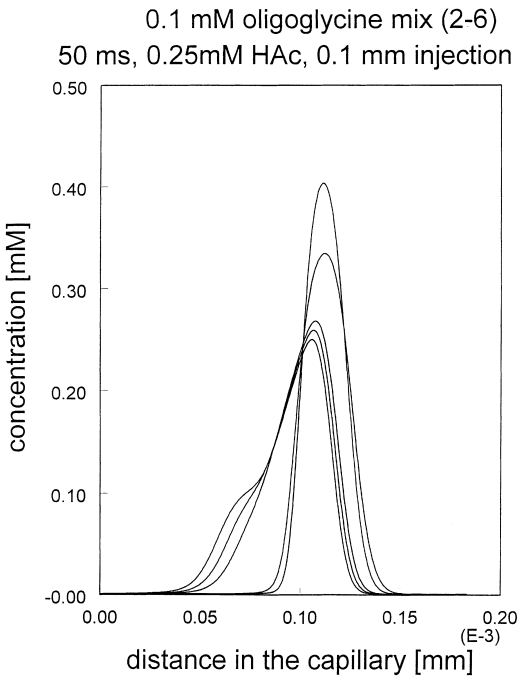

Fig. 7. A mixture of 0.1 m*M* each of 5 oligopeptides with acetic acid concentration 250 μ*M*, 100 μm pluglength, 50 ms simulation time.

The dynamic simulation proves useful for moderate stacking factors. At high stacking factors, numerical diffusion predominates, unless exponentially prolonged simulation times are found acceptable. In all examples given, simulation times were within one or a few minutes.

Acknowledgements

This work was partially supported by the Grant Agency of the Czech Republic, grant No. 203/96/K128.

References

[1] S. Hjertén, Chromatogr. Rev. 9 (1967) 122.
[2] J.L. Beckers, Thesis, Eindhoven University of Technology, Eindhoven, 1973.
[3] F.M. Everaerts, J.L. Beckers, Th.P.E.M. Verheggen, Isotachophoresis-Theory, Instrumentation and Applications, Elsevier, Amsterdam, 1976.
[4] P. Bocek, M. Deml, P. Gebauer, V. Dolník, Analytical Isotachophoresis, VCH, Weinheim, 1988.
[5] R.A. Mosher, D.A. Saville, W. Thormann, The Dynamics of Electrophoresis, VCH, Weinheim, 1992.
[6] S.F.Y. Li, Capillary Electrophoresis-Principles, Practice and Applications, Elsevier, Amsterdam, 1992.
[7] F. Kohlrausch, Ann. Phys. (Leipzig) 62 (1897) 209.
[8] V. Kašicka, Z. Prusík, P. Sázelová, J. Jirácek, T. Barth, J. Chromatogr. A 796 (1998) 211.
[9] V. Kašicka, Z. Prusík, P. Sázelová, T. Barth, E. Brynda, L. Machová, J. Chromatogr. A 772 (1997) 221.
[10] S.V. Ermakov, O. S Mazhorova, M.Y. Zhukov, Electrophoresis 13 (1992) 838.
[11] S.V. Ermakov, O.S. Mazhorova, Yu.P. Popov, Informatica 3 (1992) 173.
[12] B. Gaš, J. Vacík, I. Zelenský, J. Chromatogr. 545 (1991) 225.
[13] C. Schwer, B. Gaš, F. Lottspeich, E. Kenndler, Anal. Chem. 65 (1993) 2108.
[14] E.V. Dose, G.A. Guiochon, Anal. Chem 63 (1991) 1063.
[15] S.V. Ermakov, M.S. Bello and, P.-G. Righetti, J. Chromatogr. A661 (1994) 265.
[16] B. Gaš, J. Chromatogr. A 644 (1993) 161.
[17] S.V. Ermakov, M.Yu. Zhukov, L. Capelli, P.-G. Righetti, Anal. Chem. 66 (1994) 4034.
[18] J.H.P.A. Martens, J.C. Reijenga, J.H.M. ten Thije Boonkkamp, R.M.M. Mattheij, F.M. Everaerts, J. Chromatogr. A 772 (1997) 49.
[19] J.C. Reijenga, E. Kenndler, J. Chromatogr. A 659 (1994) 403.
[20] J.C. Reijenga, E. Kenndler, J. Chromatogr. A 659 (1994) 417.
[21] Landolt–Börnstein's Zahlenwerte und Funktionen aus Physik, Chemie, Astronomie, Geophysik und Technik, Vol. 2, Part 7, Springer Verlag, Berlin, 1960.
[22] T. Hirokawa, N. Nishimo, N. Aoki, Y. Kiso, Y. Sawamoto, T. Yagi, J.-I. Akiyama, J. Chromatogr. 271 (1983) D1.
[23] M.A. Survay, D.M. Goodall, S.A.C. Wren, R.C. Rowe, J. Chromatogr. A 741 (1996) 99.